The 8th International Supercritical CO_2 Power Cycles Symposium
February 27 – 29, 2024, San Antonio, Texas
Paper #111

Thermodynamic Analysis of Five Allam sCO_2 Power Cycle Configurations

Duoli Chen
Graduate Researcher
University of Pennsylvania
Philadelphia, Pennsylvania

John P. O'Connell
Professor Emeritus
University of Virginia
Charlottesville, Virginia

Warren D. Seider
Professor
University of Pennsylvania
Philadelphia, Pennsylvania

ABSTRACT

The semi-closed Allam supercritical carbon dioxide (sCO_2) cycle combusts natural gas for power generation and produces high-purity and high-pressure sCO_2 for direct sequestration or as feed for chemical synthesis. Its original configuration has higher efficiency than a combined cycle with carbon capture. However, the Allam cycle has yet to be fully optimized. This presentation explores the original and four systems using process simulation with an analysis based on lost work (entropy generation). The goal is to find process improvements that increase the overall thermodynamic efficiency as well as expose the process units that have the greatest irreversibilities. The combustor, heat exchanger, and turbine are found to have the greatest lost work, mainly due to large temperature differences in the flowing streams. Some changes to these units can increase their efficiencies, but we find that varying process configurations also yields significant improvements. In addition to the original Allam cycle, the modifications we have studied using Aspen Plus® V11 simulations are to: 1) use liquid natural gas instead of compressed natural gas as the feed, 2) omit a large CO_2 compressor for recompression, 3) install a reheat combustor before an additional gas turbine, and 4) use an externally-fired gas turbine (EFGT) for power generation. In the EFGT the turbine inlet is indirectly heated by the product of oxy-fuel combustion. This allows for higher temperatures at the turbine inlet and in the combustor. We find the EFGT system has 25.6 MW less total lost work and 4 % higher efficiency than the original Allam cycle.

INTRODUCTION

The greenhouse effect, caused by the rising atmospheric CO_2 concentration, has been an increasing concern. Global CO_2 emissions from combustion and industrial processes have risen to a new all-time high of 36.8 Gt in 2022, about four times that in 1960 [1]. The power sector is the largest source of emissions, accounting for 40 percent of total emissions. The main barrier to carbon sequestration and capture (CSC) for power plants is the high cost of additional carbon capture processes. The U.S. government has announced its Carbon Neutral target by the end of 2030. The Inflation Reduction Act of 2022 extends CSC tax credits, encourages the development of CSC technology, and makes CSC more promising for wider application.

The Allam cycle, characterized by high efficiency and near-zero emissions [2], [3], is a promising development for advanced power generation using natural gas (NG). Post oxy-combustion flue gas to generate electrical power by direct inlet to the inlet from the combustor. The gas is then dehydrated to provide pressurized CO_2 at high purity, which can be sequestered in underground cavities or supplied for industrial use, such as the production of high-value hydrocarbons or partially oxygenated chemicals. In addition, using supercritical CO_2 as the power cycle working fluid, the heat transfer pinch points of condensing steam are avoided. Among all existing oxy-fuel cycles with CSC, the Allam cycle is assessed to be the most environmentally friendly and economically feasible [4]. A 50 MW demonstration plant was constructed in La Porte, Texas by NET Power, which exclusively licenses this technology and is committed to its commercialization [5]. The first utility-scale plant providing approximately 300 MW of carbon-free electricity has been announced for Odessa, Texas, and is expected to launch operation in 2026 [6].

Work has been done to improve and optimize the Allam cycle, including parametric studies and numerical optimization [7], [8]. These modifications primarily focus on the state of the energy source, attempting to utilize the coolth from liquid fuel by switching from gaseous NG to liquefied natural gas (LNG) [9]. Another option increased the overall efficiency by raising the turbine outlet pressure, so as to avoid a large compressor [10]. A reconfiguration involved a reheating structure to extract more power from fuel [11]. These proposed variants have not yet been compared systematically from a thermodynamic approach, which best compares their performances.

In addition to analyzing existing modifications, we study a reconfiguration of the Allam cycle that involves an externally-fired gas turbine (EFGT) system. In the EFGT, the turbine inlet is indirectly heated by the product of the combustion chamber [12]. While traditional directly-fired gas turbines (DFGT) accept only clean fuel to avoid fouling, EFGTs are more adaptable to various fuels, including dirty coal, wind, solar power, nuclear, and biomass [13].

Thus, the objectives of this study are to:

- Apply a second-law analysis to current modifications of the Allam cycle to compare their overall thermodynamic and electrical efficiencies.

- Analyze the performance of a novel EFGT design.

METHODOLOGY

Second-Law Analysis rigorously assesses chemical process efficiency. It takes into account not only the quantity of energy, as covered by the First Law of Thermodynamics, but also the quality of energy in terms of the *availability* or *exergy functions* or their loss in terms of *lost work* or *entropy generation*. Such Second-Law formulations have been published in the literature and textbooks, such as by Seider et al. [14], whose notation we adopt.

For an open system, the First Law of Thermodynamics provides the energy conservation principle. The energy balance for a steady-state control volume is:

$$\Delta(\dot{m}H)_{\mathrm{fs}} = \dot{Q}_0 + \sum_i \dot{Q}_i - \sum_i \dot{W}_i \tag{1}$$

where $\Delta(\dot{m}H)_{\mathrm{fs}}$ is the sum of the enthalpy flows leaving the system minus the sum of those

entering the system, $\dot{Q}_0$ is positive for heat transfer from the surroundings, $\dot{Q}_i$is positive for heat transfer from heat reservoirs *i*, and $\dot{W}$ is positive for work *i* done by the system on the surroundings.

The electrical or power efficiency, η_{el}, is the ratio of net output power to the total energy supplied by fuel. It is an indication of the efficiency for power cycles:

$$\eta_{\mathrm{el}} = \frac{\sum_i \dot{W}_i}{\dot{m}_{\mathrm{fuel}}(\mathrm{LHV})} \tag{2}$$

where $\sum_i \dot{W}_i$ is the net power output of the cycle, $\dot{m}_{\mathrm{fuel}}$ is the inlet mass flow rate of fuel, and LHV represents the lower heating value of fuel.

The Second Law of Thermodynamics provides a relationship between heat and entropy flows for the control volume at steady state:

$$\Delta(\dot{m}S)_{\mathrm{fs}} - \frac{\dot{Q}_0}{T_0} - \sum_i \frac{\dot{Q}_i}{T_i} = \Delta\dot{S}_{\mathrm{irr}} \tag{3}$$

where $\Delta(\dot{m}S)_{\mathrm{fs}}$ is the sum of the entropy flows leaving the control volume minus the sum of those entering the control volume, $-\frac{\dot{Q}_0}{T_0}$ is entropy flow transferred to the surroundings at an environmental absolute temperature T_0, $-\frac{\dot{Q}_i}{T_i}$ is entropy flow transferred to heat reservoir *i* at T_i, and $\Delta\dot{S}_{\mathrm{irr}}$ is the rate of increase in entropy of the control volume due to irreversibilities; it is often identified as the entropy generation.

Multiplying Eq. (3) by T_0, and subtracting the result from Eq. (1), gives:

$$\Delta[\dot{m}(H - T_0 S)]_{\mathrm{fs}} - \sum_i \dot{Q}_i \left(1 - \frac{T_0}{T_i}\right) + \sum_i \dot{W}_i + T_0 \Delta\dot{S}_{\mathrm{irr}} = 0 \tag{4}$$

To facilitate the interpretation of entropy-related terms with their physical nature, the *availability function,* or equivalently*, exergy*, *B,* is a combination of enthalpy and entropy. It is defined as:

$$\dot{B} = \dot{H} - T_0 \dot{S} \tag{5}$$

Lost Work (LW), is defined to account for the generation of entropy:

$$L\dot{W} = T_0 \Delta\dot{S}_{\mathrm{irr}} \tag{6}$$

By substituting the defined functions, Eq. (4) can be rewritten and rearranged as:

$$L\dot{W} = -\sum_i \dot{W}_i - \Delta[\dot{m}(B)]_{\mathrm{fs}} + \sum_i \left(1 - \frac{T_0}{T_i}\right)\dot{Q}_i \tag{7}$$

If a process is reversible and adiabatic, *i.e*. isentropic, the maximum work that can be extracted from the process equals the change in availability/exergy of the flowing streams. Lost work is the loss of availability or exergy due to entropy generation within the system or heat exchange with the environment over a finite temperature difference. The rate of lost work can be calculated

from Eq. (7) for a whole process or for each of its units. The thermodynamic efficiency is given by:

$$\eta_{\mathrm{II}} = \frac{\text{main goal}}{\text{main goal} - L\dot{W}} \tag{8}$$

where, as indicated in Table 1, each term on the right-hand side of Eq. (7) could be the main goal of Eq. (8).

Table 1 Possible Main Goals of an Operation or Process [14]

Main Goal	Explanation
$-\sum_i \dot{W}_i$	Work transfer
$-\Delta[\dot{m}(B)]_{\mathrm{fs}}$	Change in availability function of flowing streams
$\sum_i \left(1 - \frac{T_0}{T_i}\right)\dot{Q}_i$	Work equivalent of heat transfer

Reducing the rate of lost work will increase efficiency regardless of which main goal is chosen. In this work, the main goal is the total net power output from the cycle, $-\sum_i \dot{W}_i$. Then the thermodynamic efficiency is:

$$\eta_{\mathrm{II}} = \frac{-\sum_i \dot{W}_i}{-\sum_i \dot{W}_i - L\dot{W}} \tag{9}$$

CYCLE DESCRIPTIONS

Four Common Variants of Allam Cycle

The main features of the Allam Cycle are shown in the block diagram of Figure 1. The Allam cycle employs NG as its fuel and highly pure oxygen from an air separation unit (ASU) as oxidant. Together with pressurized high purity sCO_2 flow, oxyfuel combustion takes place in the combustion chamber. The flue gas expands in the turbine to generate electricity and releases heat in the recuperator. All of the water and part of the CO_2 are removed. The resulting nearly pure CO_2 is compressed and pumped before receiving heat in the recuperator for the next round of the cycle. A common modification of the Allam cycle is to feed LNG instead of gaseous fuel. In this study, the Propane Precooled Mixed Refrigerant LNG Process cycle is selected as the default method for the production of LNG [15].

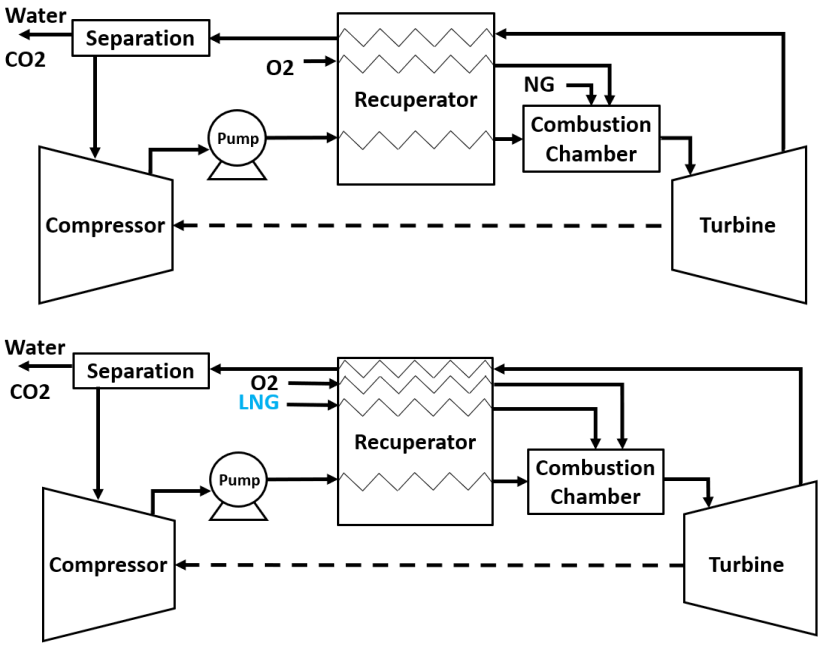

Figure 1 Block diagram of the original Allam cycle (above) and the Allam cycle with LNG (below)

An alternative modification is to change the turbine outlet pressure in order to omit the compressor, as shown in Figure 2. After separation, the high purity CO_2 is condensed and separated at low temperature, followed by pressurization. Finally, a reheating configuration has been extensively explored [11]. After the first turbo-expansion, the flue gas goes through a second round of oxy-fuel combustion and turbo-expansion. The inlets for both combustion chambers are identical.

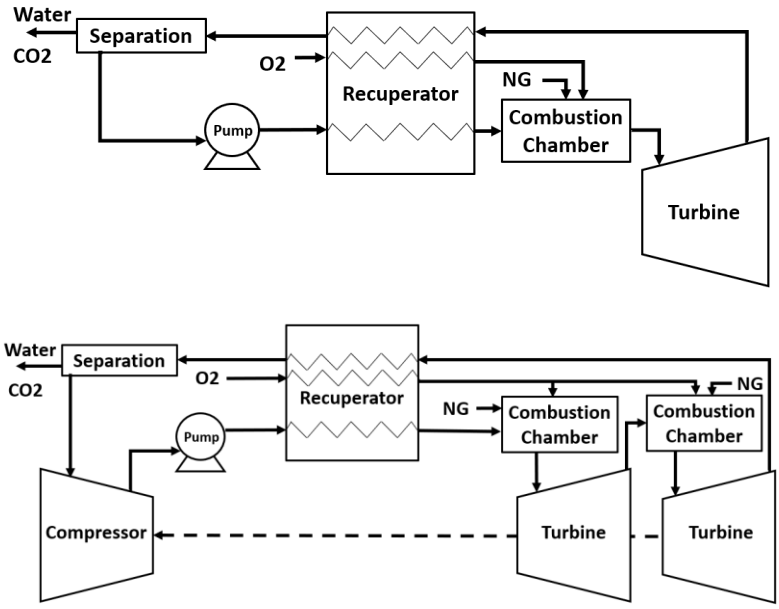

Figure 2 Block diagram of the Allam cycle without recompression (above) and the Allam cycle with reheating (below)

A sCO_2 cycle with EFGT

The four cycles described above can be categorized as directly fired cycle, where working fluid directly receives heat in the combustion chamber. In contrast, in the externally fired configuration, working fluid receives heat from oxy-fuel combustion indirectly in heat exchanger, as shown in Figure 3. The heated working fluid expands in the turbine, before absorbing heat in from combustion. The EFGT design is able to employ dirty coal or biomass as the fuel is not directly connected to the turbine.

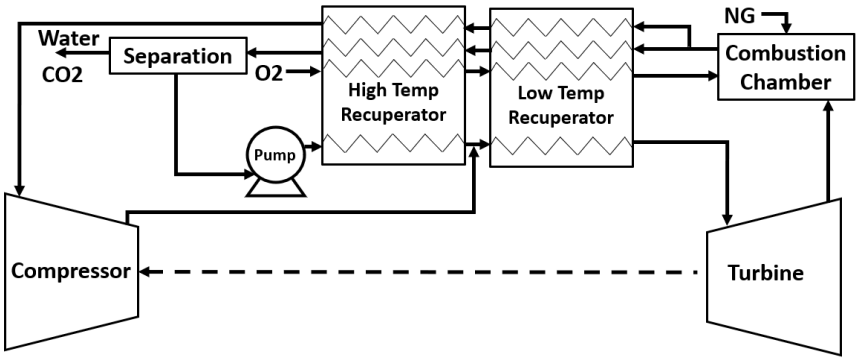

Figure 3 Block diagram of externally fired cycle

Herein, the novel EFGT sCO_2 cycle is shown in Figure 4. The oxygen stream (stream 1A) is pressurized before receiving heat in the three heat exchangers (LO2HX, RECL, RECH) in series. The natural gas feed (stream 1B) is compressed before reacting stoichiometrically with the hot oxygen (stream 5A) and mixed with high-purity CO_2 in the combustion chamber (CC). The flue gas (stream 6) releases heat in both a high- and a low-temperature recuperator before its water is mostly removed in separator (SEP) at 76 °C. The high-purity CO_2 (stream 10) is split into a bypass stream (stream 17) and a main stream (stream 11) which is cooled to room temperature to condense the CO_2. Some of CO_2 leaves the system in stream 13 while the remainder (stream 15) is pressurized in a pump (CO2PUMP) and heated in the recuperators. The bypass stream is compressed, mixed with the RECL outlet stream (stream 16) from the recuperator RECL, and fed to recuperator RECH to be further heated. The high temperature sCO_2 stream is expanded in the turbine (TB) before reentering the CC to be heated indirectly from the oxy-fuel combustion.

The simulations were conducted with Aspen Plus® v11 and with the equation of state SRKKD selected as the property method to obtain the energies, entropies, heats, and works of Eq. (1) – (9). It is expected that property errors of the equation of state will cancel out in the comparisons among the processes. The principal process values are listed in Table 2.

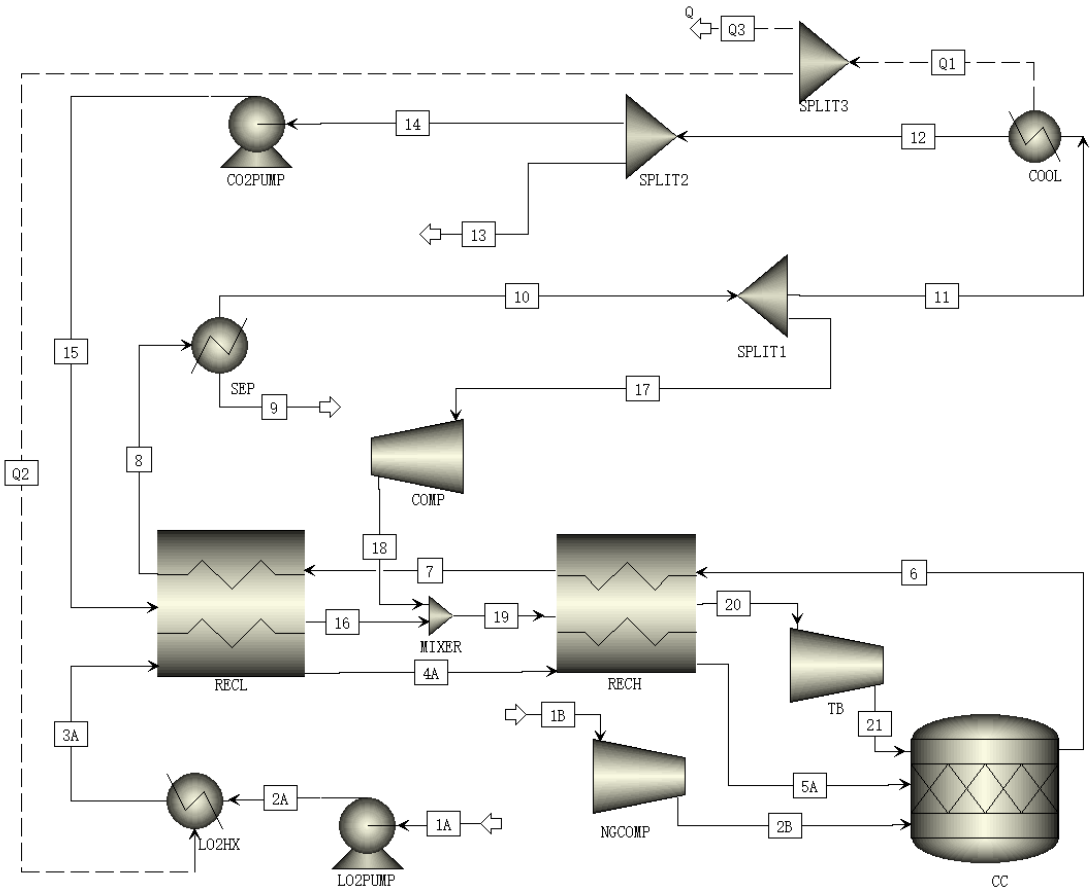

Figure 4 Process flow diagram of EFGT cycle

Table 2 Process Parameters

Process Parameter	Value
Turbine inlet temperature (°C)	1154
Turbine inlet pressure (MPa)	30
Total mass flow rate of fuel (kg/s)	12
Minimum approach temperature (°C)	10
Pressure drop across recuperator (%)	2
Isentropic efficiency of compressor (%)	85
Isentropic efficiency of turbine (%)	85
Isentropic efficiency of pump (%)	80
Power generation efficiency (%)	99.5

RESULTS AND DISCUSSION

Table 3 lists the process performance results. Note that since the mass rate of fuel is the same for all cases, lower electrical efficiency means less work is produced. The Allam cycle without recompression has the highest efficiency of the current configurations by avoiding the inefficient compressor in the design. The Allam cycles with LNG and with reheating are not as efficient as the original configuration. The novel EFGT cycle is calculated to have the highest efficiency, four percent higher than the original cycle.

Table 3 Electrical and Thermodynamic Efficiencies for Each Cycle

Cycle name	Net Cycle Power (MW)	Lost Work (MW)	Electrical Efficiency (%)	Thermodynamic Efficiency (%)
Original Allam Cycle	338.9	262.8	60.7	56.3
Allam Cycle with LNG	328.5	273.0	58.9	54.6
Allam Cycle Without Recompression	348.0	253.7	62.4	57.8
Allam Cycle with Reheating	336.2	265.7	60.3	55.9
EFGT Cycle	359.1	237.2	64.4	60.2

Using Second-Law analysis, the lost work from each equipment unit is visualized in Figure 5. The combustor has the largest lost work in all of the processes, accounting for up to 60% of the total. The second largest lost work generator in most of the processes is the recuperator, where there are large temperature differences in the heat exchangers. Next most lost work is in the turbines.

In the Allam cycle with LNG, the lost work generated in the liquefaction has been included. While this process allows waste heat recovery, the overall thermodynamic efficiency is not improved because there is more lost work generated by the large temperature difference between the hot flue gas and the cold LNG than recovered elsewhere. In the Allam cycle without compression, there is greater heating duty and lost work in the CO_2 pump, but the total lost work is actually reduced. In the Allam cycle with reheating configuration, the lost work from the recuperators is decreased by the reduced mass flow rate of recycled working fluid, but the lost work from the CO_2 compressor is twice as much as that in the original cycle, due to its higher pressure ratio. This gives more total lost work than for the original design.

We find that the EFGT system has the smallest lost work. The externally-fired design allows the combustion chamber to operate at a higher temperature, which reduces its loss work. Also since only part of the recycled CO_2 is pressurized and condensed before being pumped to high pressure, reducing the lost work in the heat exchangers. It is likely that further optimization can be found through further studies.

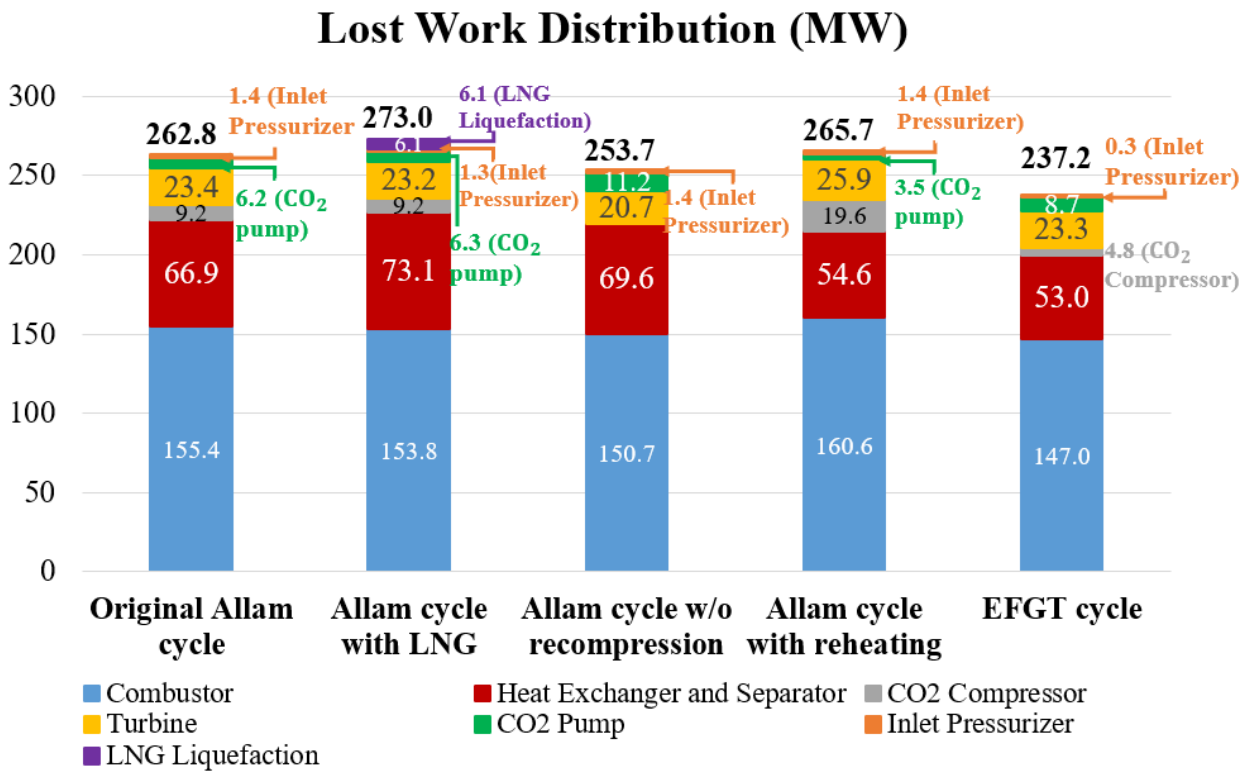

Figure 5 Lost work distribution of five cycles

CONCLUSIONS

In this study, the efficiencies of four common variants of the Allam cycle and a novel reconfiguration with EFGT are compared using a second law analysis based on lost work. This thermodynamic approach identifies both the highest overall efficiency as well as that of each equipment unit. The EFGT cycle has the highest thermodynamic and electrical efficiencies, while the current Allam cycle without CO_2 recompression is significantly less efficient. The configurations with LNG and reheating are not even as efficient as the original Allam cycle design. Further investigation of the EFGT configuration is suggested.

ACKNOWLEDGEMENTS

The research received no external funding.

REFERENCES

[1] "CO2 Emissions in 2022," IEA. Accessed: Jul. 01, 2023. [Online]. Available: https://www.iea.org/reports/co2-emissions-in-2022

[2] R. J. Allam *et al.*, "High efficiency and low cost of electricity generation from fossil fuels while eliminating atmospheric emissions, including carbon dioxide," *Energy Procedia*, vol. 37, pp. 1135–1149, Jan. 2013, doi: 10.1016/j.egypro.2013.05.211.

[3] R. Allam *et al.*, "Demonstration of the Allam cycle: an update on the development status of a high efficiency supercritical carbon dioxide power process employing full carbon capture,"

Energy Procedia, vol. 114, pp. 5948–5966, Jul. 2017, doi: 10.1016/j.egypro.2017.03.1731.

[4] N. Rogalev *et al.*, “Review of Closed SCO_2 and Semi-Closed Oxy–Fuel Combustion Power Cycles for Multi-Scale Power Generation in Terms of Energy, Ecology and Economic Efficiency,” *Energies*, vol. 15, no. 23, p. 9226, 2022, doi: 10.3390/en15239226.

[5] S. Martin *et al.*, “Progress update on the Allam cycle: commercialization of Net Power and the Net Power femonstration facility,” *SSRN Electron. J.*, 2019, doi: 10.2139/ssrn.3366370.

[6] NET Power, “NET Power Announces its First Utility-Scale Clean Energy Power Plant Integrated with CO_2 Sequestration.” Accessed: Nov. 16, 2022. [Online]. Available: https://www.prnewswire.com/news-releases/net-power-announces-its-first-utility-scale-clean-energy-power-plant-integrated-with-co2-sequestration-301669970.html

[7] R. Scaccabarozzi, M. Gatti, and E. Martelli, “Thermodynamic analysis and numerical optimization of the NET Power oxy-combustion cycle,” *Appl. Energy*, vol. 178, pp. 505–526, Sep. 2016, doi: 10.1016/j.apenergy.2016.06.060.

[8] Y. Zhao, B. Wang, J. Chi, and Y. Xiao, “Parametric study of a direct-fired supercritical carbon dioxide power cycle coupled to coal gasification process,” *Energy Convers. Manag.*, vol. 156, pp. 733–745, Jan. 2018, doi: 10.1016/j.enconman.2017.11.044.

[9] W. Chan, H. Li, X. Li, F. Chang, L. Wang, and Z. Feng, “Exergoeconomic analysis and optimization of the Allam cycle with liquefied natural gas cold exergy utilization,” *Energy Convers. Manag.*, vol. 235, p. 113972, May 2021, doi: 10.1016/j.enconman.2021.113972.

[10] Z. Zhu, Y. Chen, J. Wu, S. Zhang, and S. Zheng, “A modified Allam cycle without compressors realizing efficient power generation with peak load shifting and CO_2 capture,” *Energy*, vol. 174, pp. 478–487, May 2019, doi: 10.1016/j.energy.2019.01.165.

[11] W. Chan, X. Lei, F. Chang, and H. Li, “Thermodynamic analysis and optimization of Allam cycle with a reheating configuration,” *Energy Convers. Manag.*, vol. 224, p. 113382, Nov. 2020, doi: 10.1016/j.enconman.2020.113382.

[12] D. Cocco, P. Deiana, and G. Cau, “Performance evaluation of small size externally fired gas turbine (EFGT) power plants integrated with direct biomass dryers,” *Energy*, vol. 31, no. 10, pp. 1459–1471, Aug. 2006, doi: 10.1016/j.energy.2005.05.014.

[13] K. A. Al-attab and Z. A. Zainal, “Externally fired gas turbine technology: A review,” *Appl. Energy*, vol. 138, pp. 474–487, Jan. 2015, doi: 10.1016/j.apenergy.2014.10.049.

[14] W. D. Seider, D. R. Lewin, J. D. Seader, S. Widagdo, R. Gani, and K. M. Ng, *Product and Process Design Principles: Synthesis, Analysis and Evaluation*, Fourth edition. Wiley, 2017.

[15] S. Mokhatab, J. Y. Mak, J. V. Valappil, and D. A. Wood, Eds., “Energy and exergy analyses of natural gas liquefaction cycles,” in *Handbook of Liquefied Natural Gas*, Boston: Gulf Professional Publishing, 2014, pp. 185–228. doi: 10.1016/B978-0-12-404585-9.00004-0.